Modeling studies of NO-γ emissions of sprites

Ningyu Liu[1] and Victor P. Pasko[1]

Received 12 April 2007; revised 13 June 2007; accepted 18 July 2007; published 21 August 2007.

[1] Motivated by observations of NO-γ emissions: $NO(A^2\Sigma^+) \rightarrow NO(X^2\Pi_r) + h\nu$ from streamer discharges in laboratory experiments, we develop a model to study these emissions associated with streamer discharges in air at different pressures. The modeling results indicate that the $NO(A^2\Sigma^+)$ species in sprite streamers at 70 km altitude are mostly produced by interaction of $N_2(A^3\Sigma_u^+)$ metastable species with high-density ambient $NO(X^2\Pi_r)$ molecules. Analysis of the production and loss mechanisms for the upper excited states leading to NO-γ and N_2 LBH emissions demonstrates that the total intensity of NO-γ emissions associated with sprites is substantially weaker than that of the N_2 LBH emissions. The same conclusion can be drawn for elves following similar analysis. It is demonstrated that the presented modeling approach and analysis are consistent with prior knowledge on NO-γ emissions from aurora, indicating that to observe the NO-γ emissions from aurora, the ambient NO density must be highly enhanced in the auroral region. **Citation:** Liu, N., and V. P. Pasko (2007), Modeling studies of NO-γ emissions of sprites, *Geophys. Res. Lett.*, *34*, L16103, doi:10.1029/2007GL030352.

1. Introduction

[2] Sprites are spectacular luminous discharges, which appear in the altitude range of ~40 to 90 km above thunderstorms [*Sentman et al.*, 1995]. Optical measurements of sprites indicate that four emission band systems of N_2 and N_2^+ appear in the sprite spectrum. They are red emissions from the first positive band system of N_2 ($1PN_2$) [e.g., *Mende et al.*, 1995; *Hampton et al.*, 1996], blue emissions of second positive band system of N_2 ($2PN_2$) and the first negative band system of N_2^+ ($1NN_2^+$) [e.g., *Armstrong et al.*, 1998; *Suszcynsky et al.*, 1998], and far-UV emissions of LBH band system of N_2 [e.g., *Mende et al.*, 2006].

[3] Telescopic imaging and high-speed video observations reveal that decameter-scale thin structures are present in sprites [e.g., *Stanley et al.*, 1999; *Gerken et al.*, 2000; *Cummer et al.*, 2006; *McHarg et al.*, 2007; *Stenbaek-Nielsen et al.*, 2007], which are in a good agreement with the streamer mechanism of sprites [*Pasko*, 2007, and references therein].

[4] Spectroscopic studies of sprites provide insightful information about the sprite discharges. After analyzing simultaneous recordings of various emission band systems of sprites by the ISUAL instrument on the FORMOSAT-2 satellite, *Kuo et al.* [2005] conclude that the strength of the driving electric field, and the mean energy of electrons in sprites are ~3 times of the conventional breakdown field of air, and 6.2–9.2 eV, respectively, consistent with streamer modeling results. These results are further supported by the direct comparison of intensity ratios of different emissions in the ISUAL spectrophotometric data with modeling results on sprite streamer emissions [*Liu et al.*, 2006].

[5] The study presented in this paper is motivated by spectroscopic work on streamer discharges in laboratory experiments [e.g., *Tochikubo and Teich*, 2000; *Ono and Oda*, 2005]. In laboratory experiments N_2 LBH emissions are generally obscured by the strong emissions of NO-γ system: $NO(A^2\Sigma^+) \rightarrow NO(X^2\Pi_r) + h\nu$ [e.g., *Teich*, 1993; *Tochikubo and Teich*, 2000], the wavelengths of which are in the range of 200–290 nm. The purpose of this paper is to discuss NO chemistry in low pressure streamer discharges as applicable to sprite phenomenon and to report quantitative modeling results on NO-γ emissions from sprite streamers.

2. Model Formulation

[6] The streamer model equations used in this study are the same as in the work by *Liu and Pasko* [2004], and the simulation domain is identical to the one of *Liu and Pasko* [2005, Figure 1b]. A chemical model to study NO chemistry in streamers is solved simultaneously with the streamer model. This model includes 10 neutral species: N_2, O_2, $N(^2D)$, $N(^4S)$, $O(^3P)$, $N_2(A^3\Sigma_u^+)$, $N_2(B^3\Pi_g)$, $N_2(C^3\Pi_u)$, $NO(X^2\Pi_r)$, and $NO(A^2\Sigma^+)$. Important reactions for NO chemistry and NO-γ emissions are listed in Table 1.

[7] The direct excitation of $NO(A^2\Sigma^+)$ by electron impact is negligible, and these species are excited mainly through resonant energy transfer: $N_2(A^3\Sigma_u^+) + NO(X^2\Pi_r) \rightarrow NO(A^2\Sigma^+) + N_2(X^1\Sigma_g^+)$, where $N_2(A^3\Sigma_u^+)$ is a metastable state [*Simek*, 2002, and references therein]. $N_2(A^3\Sigma_u^+)$ has a relatively low excitation energy threshold ~6 eV and a lifetime of 2 s [*Simek*, 2003]. An important role is played by $N_2(A^3\Sigma_u^+)$ in the streamer discharges, especially in the post-discharge period, including population of the upper excited states leading to $1PN_2$ and $2PN_2$ emissions by energy pooling reactions, and by generating free electrons through reaction with N_2 singlet metastables [e.g., *Guerra et al.*, 2001; *Simek*, 2003]. The NO-γ emission is frequently used to monitor the evolution of $N_2(A^3\Sigma_u^+)$ species [*Simek et al.*, 1998].

[8] For streamer discharges in N_2/O_2 mixtures, NO is produced by the reaction: $N(^2D) + O_2 \rightarrow NO(X^2\Pi_r) + O(^3P)$. The species $N(^2D)$ are generated by electron impact dissociation of N_2 molecules. There is a lack of studies on dissociation cross sections of N_2 by electron impact in the energy range from the threshold (~10 eV) to several tens eV. We assume that $N(^2D)$ and $N(^4S)$ atoms are generated with

[1]Communications and Space Sciences Laboratory, Department of Electrical Engineering, Pennsylvania State University, University Park, Pennsylvania, USA.

0094-8276/07/2007GL030352$05.00

Table 1. List of Reactions Important for NO-γ Emissions

Reaction Process or Index	Reaction	Rate Coefficient and References[a]
	Electron Collision Reactions	
1	$e + N_2 \rightarrow e + N(^4S) + N(^2D)$	$f(E/N)$ [*Benilov and Naidis*, 2003; *Zipf and McLaughlin*, 1978]
2	$e + O_2 \rightarrow e + O(^3P) + O(^3P)$	$f(E/N)$ [*Benilov and Naidis*, 2003]
3	$e + N_2 \rightarrow e + N_2(A^3\Sigma_u^+)$	$f(E/N)$ [*Aleksandrov et al.*, 1995]
4	$e + N_2 \rightarrow e + N_2(B^3\Pi_g)$	$f(E/N)$ [*Moss et al.*, 2006]
5	$e + N_2 \rightarrow e + N_2(C^3\Pi_u)$	$f(E/N)$ [*Moss et al.*, 2006]
6	$e + NO(X^2\Pi_r) \rightarrow e + NO(A^2\Sigma^+)$	$f(E/N)$ [*Simek*, 2002]
	Chemical Reactions	
7	$N(^2D) + O_2 \rightarrow NO(X^2\Pi_r) + O(^3P)$	5.20×10^{-18} m^{3}s^{-1} [*Zhao et al.*, 2005]
8	$N_2(A^3\Sigma_u^+) + O(^3P) \rightarrow NO(X^2\Pi_r) + N(^2D)$	7×10^{-18} m^{3}s^{-1} [*Guerra et al.*, 2001]
9	$N(^2D) + NO \rightarrow N_2 + O(^3P)$	6.0×10^{-17} m^{3}s^{-1} [*Zhao et al.*, 2005]
	Excitation	
10	$N_2(A^3\Sigma_u^+) + NO(X^2\Pi_r) \rightarrow NO(A^2\Sigma^+) + N_2(X^1\Sigma_g^+)$	8.75×10^{-17} m^{3}s^{-1} [*Simek*, 2003]
	Quenching	
11	$N(^2D) + N_2 \rightarrow N(^4S) + N_2$	1.70×10^{-20} m^{3}s^{-1} [*Zhao et al.*, 2005]
12	$N_2(A^3\Sigma_u^+) + O_2 \rightarrow N_2 + O_2$	8.75×10^{-19} m^{3}s^{-1} [*Guerra et al.*, 2001]
13	$N_2(A^3\Sigma_u^+) + O_2 \rightarrow N_2 + 2O(^3P)$	1.63×10^{-18} m^{3}s^{-1} [*Guerra et al.*, 2001]
14	$NO(A^2\Sigma^+) + O_2 \rightarrow NO(X^2\Pi_r) + O_2$	1.62×10^{-16} m^{3}s^{-1} [*Simek*, 2003]
	Radiative Transition	
15	$N_2(B^3\Pi_g) \rightarrow N_2(A^3\Sigma_u^+) + h\nu$	1.7×10^5 s^{-1}[*Liu and Pasko*, 2004]
16	$N_2(C^3\Pi_u) \rightarrow N_2(B^3\Pi_g) + h\nu$	2.0×10^7s^{-1}[*Liu and Pasko*, 2004]
17	$NO(A^2\Sigma^+) \rightarrow NO(X^2\Pi_r) + h\nu$	5×10^6 s^{-1} [*Simek et al.*, 1998]

[a]Here $f(E/N)$ denotes function of reduced electric field; neutral temperature is 300 K.

an approximately equal ratio by electron collisions in this energy range [*Zipf and McLaughlin*, 1978].

[9] The natural lifetime of $NO(A^2\Sigma^+)$ is $\sim$0.2 μs, and these species are mainly quenched by O_2 with a coefficient 1.62×10^{-16} m^3/s [*Simek*, 2003]. The resulting quenching altitude is $\sim$35 km that is much lower than that of $N_2(a^1\Pi_g)$ state leading to LBH N_2 emissions ($\sim$77 km [*Liu and Pasko*, 2005, and references therein]).

3. Results and Discussion

[10] Before presenting modeling results on streamers developing at sprite altitudes, it is worthwhile to analyze the relative production rates of $NO(A^2\Sigma^+)$ and $N_2(a^1\Pi_g)$ excited molecules using similarity relations. It is known that the streamer timescales and electron density approximately scale with the air density (N) as $\sim N^{-1}$ and $\sim N^2$ [*Liu and Pasko*, 2004]. Table 2 summarizes the scaling laws for the reaction rates and product densities of several reactions leading to production of $NO(A^2\Sigma^+)$ shown in Table 1 and $N_2(a^1\Pi_g)$ molecules. As an example, the densities of the two reactants of reaction 1 scale with N as $\sim N^2$ and $\sim N$, respectively. The resulting reaction rate scales as $\sim N^3$, and the density of the products scales as $\sim N^2$ due to N^{-1} scaling of timescales for streamers. For the same composition of air, it is expected that the relative produced density of $NO(A^2\Sigma^+)$ ($\sim N^3$) with respect to $N_2(a^1\Pi_g)$ ($\sim N^2$) molecules is lower for streamers at lower pressures than those at high pressures. In addition to production, the quenching effects (discussed below) are very important for derivation of quantitative information about time dynamics of $NO(A^2\Sigma^+)$ and $N_2(a^1\Pi_g)$ densities. The above similarity analysis assumes that there is no background density of NO, and from modeling results presented below it appears that the NO densities produced by streamer at 70 km altitude are negligible in comparison with ambient NO densities.

[11] The ambient NO is present in the upper atmosphere and its density at 70 km altitude is on the order of 10^{13}–10^{14} m^{-3} depending on particular atmospheric conditions [e.g., *Atreya*, 1981; *Kumar et al.*, 1995; *Gordley et al.*, 1996]. One study found that the NO density can be as large as 2×10^{14} m^{-3} at 70 km altitude, or about 100 ppb [*Atreya*, 1981]. We use this value as the initial density of NO for our streamer simulations at 70 km altitude. Corresponding results are shown in Figure 1. The NO density stays at this value during the whole simulation, indicating that the production of NO in the streamer is unimportant in comparison with the ambient NO density. We note that NO can be destructed by O_3 produced in corona discharges in laboratory experiments. However, estimates indicate that this destruction within the duration of $\sim$0.5 ms of the simulated streamer is negligible due to the large ambient density of NO at 70 km altitude. In the streamer channel, the densities of atomic oxygen and $N_2(A^3\Sigma_u^+)$ are much higher than the rest of species except ambient NO.

Table 2. Scaling of Densities of $NO(A^2\Sigma^+)$ and $N_2(a^1\Pi_g)$ With Air Density N

Reaction or Reaction Index	Reaction Rate	Scaling of Product
	NO-γ	
1	$\sim[e][N_2]$	$\sim N^2$
2	$\sim[e][O_2]$	$\sim N^2$
3	$\sim[e][N_2]$	$\sim N^2$
7	$\sim[N(^2D)][O_2]$	$\sim N^2$
8	$\sim[N_2(A^3\Sigma_u^+)][O(^3P)]$	$\sim N^3$
10	$\sim[N_2(A^3\Sigma_u^+)][NO(X^2\Pi_r)]$	$\sim N^3$
	N_2 LBH	
$e + N_2 \rightarrow N_2(a^1\Pi_g)$	$\sim[e][N_2]$	$\sim N^2$

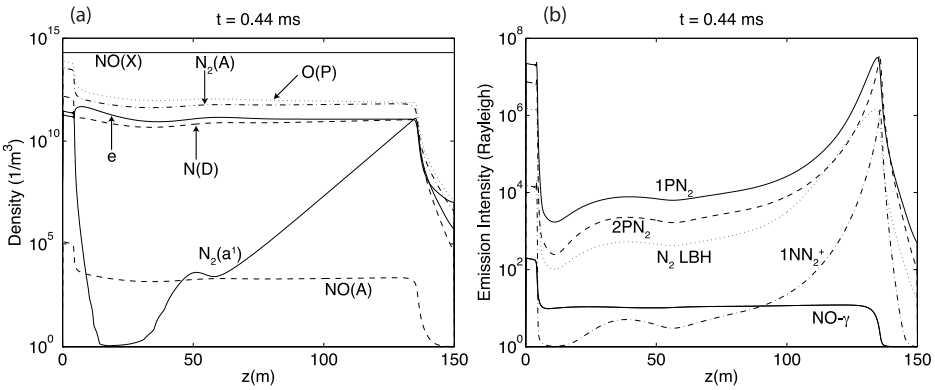

Figure 1. (a) Density profiles of various species along the central axis of the model streamer at 70 km altitude and (b) intensity profiles of emissions associated with the model streamer along the central axis. The z coordinate is aligned with the direction of the electric field.

Densities of electrons and N(^2D) are very similar. The density of $N_2(a^1\Pi_g)$ has a distribution exponentially decreasing from the streamer head to the streamer body because of the fast deactivation by radiative transition and quenching. The shape of the NO($A^2\Sigma^+$) density profile follows that of $N_2(A^3\Sigma_u^+)$ because it is produced by reaction 10 (Table 1) and the NO density is constant. For the emission intensity profiles, NO-γ emissions are approximately one order of magnitude weaker than N_2 LBH emissions in the streamer body, but stronger than $1NN_2^+$. In the streamer head, N_2 LBH emissions definitely dominate over NO-γ emissions. The relatively constant intensity ratio of NO-γ to N_2 LBH emissions in the streamer body is due to two factors: 1) Around the streamer body, there is a shell with the peak electric field about $\sim E_k$ (the conventional breakdown threshold field [see *Liu and Pasko*, 2005, Figure 2]). The $N_2(a^1\Pi_g)$ molecules excited in this shell continue to supply the N_2 LBH emissions after the $N_2(a^1\Pi_g)$ molecules produced by the passage of the streamer head are deactivated in a short time period (the lifetime of $N_2(a^1\Pi_g)$ is 14 μs at 70 km altitude [*Liu and Pasko*, 2005]); 2) The metastables $N_2(A^3\Sigma_u^+)$ in the streamer body, which are also produced by the passage of the streamer head, continuously excite NO ground state to NO($A^2\Sigma^+$) leading to NO-γ emissions. The total lifetime of $N_2(A^3\Sigma_u^+)$ at 70 km altitude accounting for quenching effects (reactions 12 and 13 in Table 1) is approximately 1 ms, which is longer than the 0.44 ms simulation time.

[12] Although the model streamer is very short, it is possible to estimate the relative strength of the total NO-γ emissions with respect to the total N_2 LBH emissions for a long streamer or even for an entire sprite event. Generally, it is expected that excitation of $N_2(A^3\Sigma_u^+)$ would be stronger than $N_2(a^1\Pi_g)$ because the excitation energy threshold for $N_2(A^3\Sigma_u^+)$ (6 eV) is lower than $N_2(a^1\Pi_g)$ (8.55 eV). However, according to Figure 2, the two excitation frequencies are very close to each other. As a matter of fact, the ratio of $N_2(A^3\Sigma_u^+)$ to $N_2(a^1\Pi_g)$ excitation frequencies varies from 2.4 to 0.6 for the electric field range of interest ($>10^6$ N/N_0 V/m, where N is the air density at the altitude under consideration and N_0 is the density at ground level). Therefore, it can be assumed, to the first order approximation, that the production of both species by electron impact reactions is on the same level in sprites, i.e., for our analysis here we assume that equal numbers of $N_2(A^3\Sigma_u^+)$ and $N_2(a^1\Pi_g)$ molecules are produced in the streamer discharges. For $N_2(A^3\Sigma_u^+)$ species, the loss processes are associated with reactions 8, 10, 12 and 13 (Table 1). Reaction 8 will be ignored in the following analysis, because the density of O(^3P) is much lower than those of NO and O_2 at 70 km altitude. Using a density of 3.83×10^{20} m^{-3} for O_2 and the density range 10^{13}–10^{14} m^{-3} for NO at 70 km altitude, the $N_2(A^3\Sigma_u^+)$ deactivation frequencies associated with reactions 10, 12 and 13 are 0.001–0.01, 335 and 624 1/s, respectively. Therefore, only about 0.0001–0.001% of produced $N_2(A^3\Sigma_u^+)$ species transfers energy to NO ground state molecules to form NO($A^2\Sigma^+$). Because the quenching altitude of NO($A^2\Sigma^+$) is much lower than 70 km, essentially all NO($A^2\Sigma^+$) molecules are deactivated by emitting NO-γ emissions. The quenching altitude of $N_2(a^1\Pi_g)$ is about 77 km. At 70 km altitude, the ratio of loss rates by radiative transition and quenching is about 1/e. Therefore, at 70 km altitude about 25% of produced $N_2(a^1\Pi_g)$ species leads to N_2 LBH emissions. Hence, the total production of NO-γ emissions is

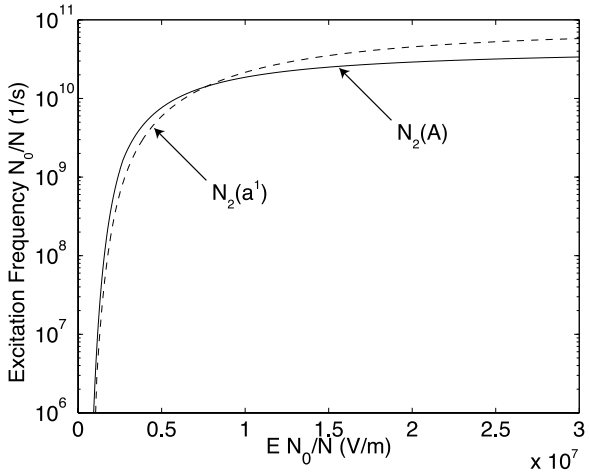

Figure 2. Excitation frequencies of $N_2(A^3\Sigma_u^+)$ [*Aleksandrov et al.*, 1995] and $N_2(a^1\Pi_g)$ [*Moss et al.*, 2006] as a function of reduced electric field. N is the air density at the altitude under consideration and N_0 is the density at ground level.

substantially weaker in comparison with N_2 LBH emissions for a streamer at 70 km altitude. Since the total intensity of N_2 LBH is more than 4 orders of magnitude greater than that of the NO-γ emissions, the NO-γ emissions from sprites are not observable for a wide bandwidth photometer such as the one used by the ISUAL instrument [*Kuo et al.*, 2005]. This result is notably different from the laboratory observations [e.g., *Teich*, 1993; *Tochikubo and Teich*, 2000], and analysis of the reasons leading to this difference will be given at the end of this paper. We note that strong bands of NO-γ emissions are located in the wavelength range 240–260 nm in which N_2 LBH emissions are absent [*Vallance-Jones*, 1974, Tables 4.14 and 4.18]. It is therefore possible that a dedicated narrow bandwidth photometer with the wavelength passband of 240–260 nm would be able to detect sprite NO-γ emissions from space (see [*Liu et al.*, 2006, Figure 3] regarding the atmospheric transmittance in this wavelength range).

[13] The same approach can be applied to analyze relative strength of NO-γ emissions to N_2 LBH emissions for elves and aurora.

[14] Assuming that the typical altitude of elves is 100 km [*Mende et al.*, 2005, and references therein], quenching processes are still the dominating loss mechanism of $N_2(A^3\Sigma_u^+)$ molecules. At this altitude, the number densities of O, NO and O_2 are 4×10^{17}, 2×10^{13} and 2.17×10^{18} $1/m^3$, respectively. The $N_2(A^3\Sigma_u^+)$ deactivation frequencies for reactions 8, 10, 12 and 13 are 2.79, 1.8×10^{-3}, 1.9 and 3.53 1/s, respectively. Therefore, only $\frac{1.8\times10^{-3}}{2.79+1.8\times10^{-3}+1.9+3.53} \times 100\% = 0.02\%$ of $N_2(A^3\Sigma_u^+)$ molecules excite $NO(X^2\Pi_r)$ leading to the NO-γ emissions. However, this altitude is higher than the quenching altitude of N_2 LBH emissions and all of excited $N_2(a^1\Pi_g)$ molecules emit. We therefore can draw a conclusion that N_2 LBH emissions are also much stronger than NO-γ emissions for elves.

[15] For aurora, we pick the altitude where the ambient NO density profile is maximum (3×10^{13} $1/m^3$ at $\sim$120 km) [*Minschwaner et al.*, 2004]. At this altitude, the number densities of O and O_2 are 7.914×10^{16} and 4.395×10^{16} $1/m^3$, respectively. The $N_2(A^3\Sigma_u^+)$ deactivation frequencies for reactions 8, 10, 12 and 13 are 0.554, 2.6×10^{-3}, 0.0385 and 0.0716 1/s, respectively. The loss of $N_2(A^3\Sigma_u^+)$ due to radiative transition (i.e., N_2 Vegard-Kaplan bands with Einstein coefficient $A_k = 0.5$ 1/s) is also important. About $\frac{2.6\times10^{-3}}{0.554+2.6\times10^{-3}+0.0385+0.0716+0.5} \times 100\% = 0.22\%$ of produced $N_2(A^3\Sigma_u^+)$ molecules excites $NO(X^2\Pi_r)$. However, it is known that NO-γ emissions have been observed from aurora [e.g., *Vallance-Jones*, 1974, p. 140]. The explanation for the observation is that ambient NO density can be enhanced in aurora and it can be as high as 10^{15} $1/m^3$ [*Viggiano and Hunton*, 1999]. If this density is used, about 7% of the total production of $N_2(A^3\Sigma_u^+)$ excites $NO(X^2\Pi_r)$. This value is on the same order as the ratio ($\frac{63}{383} \times 100\% = 16.45\%$ [*Vallance-Jones*, 1974, Tables 4.14 and 4.18]) of the total intensity of NO-γ and N_2 LBH emissions for IBC3 aurora. It should be noted that the present analysis assumes that the production of $N_2(A^3\Sigma_u^+)$ and $N_2(a^1\Pi_g)$ is mainly by electron impact excitation.

[16] We conclude by noting that strong NO-γ emissions from streamer discharges are observed in laboratory experiments [e.g., *Teich*, 1993; *Tochikubo and Teich*, 2000; *Ono and Oda*, 2005]. In those experiments, streamer discharges are generally operated in repetitive mode and the metastable molecules $N_2(A^3\Sigma_u^+)$ accumulate during a discharge period of several hundreds of ns (100 ns scales to 1.5 ms at 70 km altitude). Additionally, a large amount of background NO is commonly added to the gas medium, for example 200 ppm in the work by *Teich* [1993]. As part of this study, we simulated a positive streamer at ground pressure with a background NO density 200 ppm. The results (not shown here for the sake of brevity) indicate that NO-γ emissions are several orders of magnitude stronger than N_2 LBH emissions in the streamer body and slightly weaker in the streamer head for a positive streamer propagating up to 20 ns. The distribution of intensity of NO-γ emissions is almost constant from the streamer head to the body (similar to Figure 1b but with different magnitude). Therefore, under this kind of conditions, the overall intensity of NO-γ emissions is stronger than N_2 LBH emissions, in agreement with *Teich* [1993].

[17] **Acknowledgments.** This research was supported by NSF ATM-0134838 grant to Penn State University and by NSF CEDAR Postdoctoral Fellowship.

References

Aleksandrov, N. L., A. E. Bazelyan, E. M. Bazelyan, and I. V. Kochetov (1995), Modeling of long streamers in atmospheric-pressure air, *Plasma Phys. Rep.*, *21*(60), 57–75.

Armstrong, R. A., J. A. Shorter, M. J. Taylor, D. M. Suszcynsky, W. A. Lyons, and L. S. Jeong (1998), Photometric measurements in the SPRITES' 95 and 96 campaigns of nitrogen second positive (399.8 nm) and first negative (427.8 nm) emission, *J. Atmos. Sol. Terr. Phys.*, *60*, 787–799.

Atreya, S. K. (1981), Measurement of minor species (H_2, Cl, O_3, NO) in the Earth's atmosphere by the stellar occultation technique, *Adv. Space Res.*, *1*, 127–141.

Benilov, M. S., and G. V. Naidis (2003), Modelling of low-current discharges in atmospheric-pressure air taking account of non-equilibrium effects, *J. Phys. D Appl. Phys.*, *36*, 1834–1841, doi:10.1088/0022-3727/36/15/314.

Cummer, S. A., N. C. Jaugey, J. Li, W. A. Lyons, T. E. Nelson, and E. A. Gerken (2006), Submillisecond imaging of sprite development and structure, *Geophys. Res. Lett.*, *33*, L04104, doi:10.1029/2005GL024969.

Gerken, E. A., U. S. Inan, and C. P. Barrington-Leigh (2000), Telescopic imaging of sprites, *Geophys. Res. Lett.*, *27*, 2637–2640.

Gordley, L. L., et al. (1996), Validation of nitric oxide and nitrogen dioxide measurements made by the Halogen Occultation Experiment for UARS platform, *J. Geophys. Res.*, *101*(D6), 10,241–10,266.

Guerra, V., P. A. Sa, and J. Loureiro (2001), Role played by the $N_2(A^3\Sigma_u^+)$ metastable in stationary N_2 and N_2-O_2 discharges, *J. Phys. D Appl. Phys.*, *34*, 1745–1755.

Hampton, D. L., M. J. Heavner, E. M. Wescott, and D. D. Sentman (1996), Optical spectral characteristics of sprites, *Geophys. Res. Lett.*, *23*, 89–93.

Kumar, C. K., P. K. Swaminathan, D. E. Anderson, J.-H. Yee, M. R. Gunson, and M. C. Abrams (1995), ATMOS/ATLAS 1 measurements of thermospheric and mesospheric nitric oxide, *J. Geophys. Res.*, *100*(D8), 16,839–16,846.

Kuo, C.-L., R. R. Hsu, A. B. Chen, H. T. Su, L. C. Lee, S. B. Mende, H. U. Frey, H. Fukunishi, and Y. Takahashi (2005), Electric fields and electron energies inferred from the ISUAL recorded sprites, *Geophys. Res. Lett.*, *32*, L19103, doi:10.1029/2005GL023389.

Liu, N., and V. P. Pasko (2004), Effects of photoionization on propagation and branching of positive and negative streamers in sprites, *J. Geophys. Res.*, *109*, A04301, doi:10.1029/2003JA010064.

Liu, N., and V. P. Pasko (2005), Molecular nitrogen LBH band system far-UV emissions of sprite streamers, *Geophys. Res. Lett.*, *32*, L05104, doi:10.1029/2004GL022001.

Liu, N., et al. (2006), Comparison of results from sprite streamer modeling with spectrophotometric measurements by ISUAL instrument on FORMOSAT-2 satellite, *Geophys. Res. Lett.*, *33*, L01101, doi:10.1029/2005GL024243.

McHarg, M. G., H. C. Stenbaek-Nielsen, and T. Kammae (2007), Observations of streamer formation in sprites, *Geophys. Res. Lett.*, *34*, L06804, doi:10.1029/2006GL027854.

Mende, S. B., R. L. Rairden, G. R. Swenson, and W. A. Lyons (1995), Sprite spectra: N_2 1 PG band identification, *Geophys. Res. Lett.*, *22*, 2633–2637.

Mende, S. B., H. U. Frey, R. R. Hsu, H. T. Su, A. B. Chen, L. C. Lee, D. D. Sentman, Y. Takahashi, and H. Fukunishi (2005), D region ionization by lightning-induced electromagnetic pulses, *J. Geophys. Res.*, *110*, A11312, doi:10.1029/2005JA011064.

Mende, S. B., et al. (2006), Spacecraft based studies of transient luminous events, in *Sprites, Elves and Intense Lightning Discharges*, *NATO Sci. Ser.*, *Ser. 2*, vol. 225, edited by M. Füllekrug, E. A. Mareev, and M. J. Rycroft, pp. 123–149, Springer, Heidleberg, Germany.

Minschwaner, K., J. Bishop, S. A. Budzien, K. F. Dymond, D. E. Siskind, M. H. Stevens, and R. P. McCoy (2004), Middle and upper thermospheric odd nitrogen: 2. Measurements of nitric oxide from Ionospheric Spectroscopy and Atmospheric Chemistry (ISAAC) satellite observations of NO γ band emission, *J. Geophys. Res.*, *109*, A01304, doi:10.1029/2003JA009941.

Moss, G. D., V. P. Pasko, N. Liu, and G. Veronis (2006), Monte Carlo model for analysis of thermal runaway electrons in streamer tips in transient luminous events and streamer zones of lightning leaders, *J. Geophys. Res.*, *111*, A02307, doi:10.1029/2005JA011350.

Ono, R., and T. Oda (2005), Nitrogen oxide γ-band emission from primary and secondary streamers in pulsed positive corona discharge, *J. Appl. Phys.*, *97*, 013302.

Pasko, V. P. (2007), Red sprite discharges in the atmosphere at high altitude: The molecular physics and the similarity with laboratory discharges, *Plasma Sources Sci. Technol.*, *16*, S13–S29, doi:10.1088/0963-0252/16/1/S02.

Sentman, D. D., E. M. Wescott, D. L. Osborne, D. L. Hampton, and M. J. Heavner (1995), Preliminary results from the Sprites94 campaign: Red sprites, *Geophys. Res. Lett.*, *22*, 1205–1208.

Simek, M. (2002), The modelling of streamer-induced emission in atmospheric pressure, pulsed positive corona discharge: N_2 second positive and NO-γ systems, *J. Phys. D Appl. Phys.*, *35*, 1967–1980.

Simek, M. (2003), Determination of $N_2(A^3\Sigma_u^+)$ metastable density produced by nitrogen streamers at atmospheric pressure: 1. Design of diagnostic method, *Plasma Sources Sci. Technol.*, *12*, 421–431.

Simek, M., V. Babicky, M. Clupek, S. DeBenedictis, G. Dilecce, and P. Sunka (1998), Excitation of $N_2(C^3\Pi_u)$ and $NO(A^2\Sigma^+)$ states in a pulsed positive corona discharge in N_2, N_2-O_2 and N_2-NO mixtures, *J. Phys. D Appl. Phys.*, *35*, 2591–2602.

Stanley, M., P. Krehbiel, M. Brook, C. Moore, W. Rison, and B. Abrahams (1999), High speed video of initial sprite development, *Geophys. Res. Lett.*, *26*, 3201–3204.

Stenbaek-Nielsen, H. C., M. G. McHarg, T. Kanmae, and D. D. Sentman (2007), Observed emission rates in sprite streamer heads, *Geophys. Res. Lett.*, *34*, L11105, doi:10.1029/2007GL029881.

Suszcynsky, D. M., R. Roussel-Dupre, W. A. Lyons, and R. A. Armstrong (1998), Blue-light imagery and photometry of sprites, *J. Atmos. Sol. Terr. Phys.*, *60*, 801–809.

Teich, T. H. (1993), Emission spectroscopy of corona discharges, in *Non-Thermal Plasma Techniques for Pollution Control*, *NATO ASI Ser.*, *Ser. G*, vol. 34, part A, edited by B. M. Penetrante and S. E. Schultheis, pp. 231–248, Springer, Berlin.

Tochikubo, F., and T. H. Teich (2000), Optical emission from a pulsed corona discharge and its associated reactions, *Jpn. J. Appl. Phys.*, *39*, 1343–1350.

Vallance-Jones, A. V. (1974), *Aurora*, D. Reidel, Norwell, Mass.

Viggiano, A. A., and D. E. Hunton (1999), Airborne mass spectrometers: Four decades of atmospheric and space research at the Air Force Research Laboratory, *J. Mass Spectrom.*, *34*, 1107–1129.

Zhao, G. B., S. V. B. Garikipati, X. D. Hu, M. D. Argyle, and M. Radosz (2005), Effect of oxygen on nonthermal plasma reactions of nitrogen oxides in nitrogen, *AIChE J.*, *51*(6), 1800–1812, doi:10.1002/aic.10452.

Zipf, E. C., and R. W. McLaughlin (1978), On the dissociation of nitrogen by electron impact and by E.U.V. photo-absorption, *Planet. Space Sci.*, *26*, 449–462.

N. Liu and V. P. Pasko, CSSL, Department of Electrical Engineering, Pennsylvania State University, University Park, PA 16802, USA. (nul105@psu.edu; vpasko@psu.edu)